2014 IEEE International Conference on Robotics & Automation (ICRA)
Hong Kong Convention and Exhibition Center
May 31 - June 7, 2014. Hong Kong, China

# Physical Interaction Detection and Control of Compliant Manipulators Equipped with Friction Clutches

Navvab Kashiri, Matteo Laffranchi, Nikos G. Tsagarakis, Alessio Margan, and Darwin G. Caldwell

*Abstract*— **This work focuses on the modeling and control of robotic manipulators powered by compliant actuation systems equipped with clutches for providing friction torque on demand. A novel control scheme is proposed for modulating the clutch friction torque in this particular class of compliant actuators to make the robot operate in "Rigid mode" when it does not interact with the environment to achieve high accuracy, bandwidth and controllability; meanwhile ensuring that the robot maximum static force is constrained to a maximum threshold permitting flexible reactions in potentially risky scenarios. The robot autonomously switches to "Compliant mode" (clutches off) when it interacts with external agents to exploit the advantages of compliance during contacts. Experimental results are presented to show the effectiveness of proposed approach in improving the robot performance (tracking accuracy) while still guaranteeing an interaction-friendly behavior when contact occurs.**

## I. INTRODUCTION

Industrial robots are typically powered by actuators with high reduction gears (non-back-drivable) controlled by high gain position/velocity controllers. Such mechanical systems have high transmission stiffnesses and large reflected inertias making the robot present a inherently high output mechanical impedance. Hence, classical robots have restricted performance in terms of adaptability to different tasks and especially in their capacity to interact with various environments and humans [1]. To overcome these limitations, and inspired by humans who possess the capability to modulate the stiffness of their limb [2], series elastic actuators (SEAs) were developed to moderate the output impedance and to increase the robustness of the system [3], [4].

The use of elastic elements in robots can enhance the interaction capacity with humans and different environments [5], and has an additional benefit from the potential capability of the system to store energy [6]. However, unwanted oscillations caused by the underdamped dynamics of these robots adversely affect the stability margin and the tracking accuracy achieved by the control system [7]. Induced oscillations could be regulated using active damping control [8]. However, the stable dissipative operations that use this type of control are limited by the bandwidth of the feedback loop, and typically have phase lag problems and noise in the velocity feedback [9], [10]. Furthermore, these control methods require large control efforts leading to a significant energy cost [11].

Authors are with the Department of Advanced Robotics, Istituto Italiano di Technologia, Via Morego 30, 16163 Genoa, Italy navvab.kashiri, matteo.laffranchi, nikos.tsagarakis, alessio.margan, darwin.caldwell@iit.it

To address these issues, variable impedance actuators (VIAs) have been used to regulate the passive impedance based on the requirements of the operating conditions and tasks. A well-known type of VIAs is the Variable stiffness actuator (VSAs) which can be implemented using serial and antagonistic configurations [12]–[14]. A more recent innovation in VIAs relies upon embedding dissipation mechanisms (physical damping) in SEAs/VSAs to augment the damping ratio of the system. These actuators can use various types of dissipation systems such as friction clutches [15], viscous damping [16] and electrical inductance effects [17]. Series Clutch actuators (SCA) are another type of VIAs exploiting clutch mechanisms, instead of elastic elements, to modulate the impedance by controlling the clutch mechanism [18]. SCA systems can be also emplyed as an adjustable torque limiter for bounding the maximum external force applied by the robot [19].

This work focuses on the modeling and use of friction clutches in the actuators of a compliant manipulator arm, with the goal of achieving excellent tracking performance in a robot that can freely interact with the environment. Contact detection has been widely studied during the past decade using different approaches [20]–[22]. The contact detection approach adopted in this work is based only on monitoring the spring deflection angles of joints. The aim is to lock the transmission clutch of joints when no external object/agent presents and to intrinsically unlock them when the robot gets in contact with environment. To achieve this, the clutch torque is modeled based on the dynamics of the robot. Having developed the arm model, the clutch normal force control is formulated to modulate the transmission friction torques in such a way that the action of the elastic elements is bypassed, meanwhile the total static force exerted by the robot is limited to a maximum threshold that is set to an appropriate value based on the task requirements. This scheme is exploited for the implementation of a dual compliant/rigid mode controller to make the robot operate as a rigid robot when excellent accuracy and tracking performance is required while being intrinsically able to switch to a compliant system to take advantage of passive compliance and facilitate friendly interaction when the robot is in contact with environment.

The paper is structured as follows: the modeling of the arm is presented in Section II while Section III describes the control strategies implemented on the arm. Experimental results are presented in section IV. Finally the conclusion is addressed in section V.

978-1-4799-3684-7/14/$31.00 ©2014 IEEE

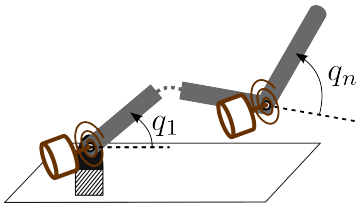


Fig. 1: Schematic of a manipulator powered by compliant actuators.

## II. Modeling

For the $n$-degrees of freedom (DOFs) serial manipulator, shown in Fig. 1 powered by compliant actuators presented in Fig. 2, the dynamic equations of the system can be expressed by [23]

$$\mathbf{M}(\boldsymbol{q})\ddot{\boldsymbol{q}} + \mathbf{D}_{\mathrm{l}}\dot{\boldsymbol{q}} + \boldsymbol{c}(\boldsymbol{q},\dot{\boldsymbol{q}}) + \boldsymbol{g}(\boldsymbol{q}) + \boldsymbol{\tau}_{\mathrm{t}} = \boldsymbol{\tau}_{\mathrm{e}}, \tag{1}$$

$$\mathbf{B}\ddot{\boldsymbol{\theta}} + \mathbf{D}_{\mathrm{m}}\dot{\boldsymbol{\theta}} - \boldsymbol{\tau}_{\mathrm{t}} = \boldsymbol{\tau}_{\mathrm{m}}, \tag{2}$$

where $\boldsymbol{\theta} = [q_1, ..., q_n]^T$ and $\boldsymbol{q} = [\theta_1, ..., \theta_n]^T$ denote the vectors of the generalized motor and link positions, respectively; $\mathbf{M} \in \Re^{n\times n}$ and $\mathbf{D}_{\mathrm{l}} \in \Re^{n\times n}$ show the inertia and damping matrix associated with the link side; $\mathbf{B} = diag(B_1, ..., B_n)$ and $\mathbf{D}_{\mathrm{m}} = diag(D_{\mathrm{m},1}, ..., D_{\mathrm{m},n})$ indicate the diagonal inertia and viscous damping matrices related to the motor side; $\boldsymbol{g} \in \Re^n$ and $\boldsymbol{c} \in \Re^n$ are the vectors of gravity terms and coriolis/centrifugal terms of the link; $\boldsymbol{\tau}_{\mathrm{m}} \in \Re^n$ and $\boldsymbol{\tau}_{\mathrm{e}} \in \Re^n$ are the vectors of torques applied by the motors and external objects/agents; and $\boldsymbol{\tau}_{\mathrm{t}} = [\tau_{\mathrm{t},1}, ..., \tau_{\mathrm{t},n}]^T$ is the vector of transmission torques applied by passive elastic elements and clutch mechanisms which can be computed as

$$\boldsymbol{\tau}_{\mathrm{t}} = \mathbf{D}_{\mathrm{t}}(\dot{\boldsymbol{q}} - \dot{\boldsymbol{\theta}}) + \mathbf{K}_{\mathrm{t}}(\boldsymbol{q} - \boldsymbol{\theta}) + \boldsymbol{\tau}_{\mathrm{c}}, \tag{3}$$

where $\mathbf{K}_{\mathrm{t}} = diag(K_{\mathrm{t},1}, ..., K_{\mathrm{t},n})$ shows the diagonal matrix of the transmission stiffness, $\mathbf{D}_{\mathrm{t}} = diag(D_{\mathrm{t},1}, ..., D_{\mathrm{t},n})$ is the inherent viscous damping matrix, and $\boldsymbol{\tau}_{\mathrm{c}} = [\tau_{\mathrm{c},1}, ..., \tau_{\mathrm{c},n}]^T$ is the vector of friction torques applied by the clutch.

To model the friction torque applied by the clutch, two operating conditions are considered: One for the clutch locked and another for the clutch unlocked (slipping). In the case where there is relative motion between the clutch surfaces, i.e. unlocked, the torque generated by the corresponding clutch can be modeled as dynamic coulomb friction torque. However, when the clutch of a joint is locked, the torque applied by the clutch is modeled as static friction.

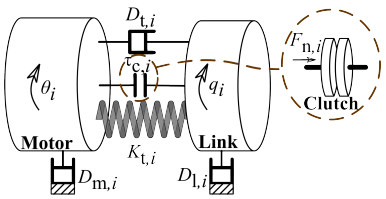


Fig. 2: Schematic of a compliant actuator equipped with transmission clutch.

In case $u_{\mathrm{n}}$ joints are unlocked, $\dot{q}_i \neq \dot{\theta}_i$ for $i = u_1, ..., u_{\mathrm{n}}$ where $u_{\mathrm{n}} \leq n$, the $i$th clutch torque is modeled as dynamic friction torque which can be obtained by

$$\tau_{\mathrm{df},i} = F_{\mathrm{n},i}\mu_{\mathrm{s},i}R_i sgn(\dot{q}_i - \dot{\theta}_i), \tag{4}$$

where $F_{\mathrm{n},i}$ is the clutch normal force, $\mu_{\mathrm{d},i}$ is the dynamic coulomb friction coefficient, and $R_i$ is a geometrical constant factor depending on the shape and size of friction interface associated with $i$th joint ($sgn(.)$ is the signum function). The geometrical parameter can be obtained from the following equation for circular shape interfaces

$$R_i = \frac{a_i^3 - b_i^3}{a_i^2 - b_i^2}, \tag{5}$$

where $a_i$ and $b_i$ are the diameters of the outer and inner rings of the friction interfaces of $i$th joint, respectively.

When $l_{\mathrm{n}}$ joints are locked, where $l_{\mathrm{n}} + u_{\mathrm{n}} = n$, the clutch friction torque associated with these joints needs to be derived from the dynamics of system. Extracting angular acceleration vector of links and motors from the dynamic equations of the arm (1) and (2), it can be written that

$$\ddot{\boldsymbol{q}} - \ddot{\boldsymbol{\theta}} + \mathbf{H}\boldsymbol{\tau}_{\mathrm{c}} = \boldsymbol{P}(\boldsymbol{q}, \boldsymbol{\theta}, \dot{\boldsymbol{q}}, \dot{\boldsymbol{\theta}}), \tag{6}$$

where $\mathbf{H} = (\mathbf{M}^{-1} + \mathbf{B}^{-1})$ and the auxiliary vector $\boldsymbol{P} \in \Re^n$ is defined by

$$\begin{aligned}\boldsymbol{P} = {} & \mathbf{M}^{-1}(\boldsymbol{\tau}_{\mathrm{e}} - \mathbf{D}_{\mathrm{l}}\dot{\boldsymbol{q}} - \boldsymbol{c}(\boldsymbol{q},\dot{\boldsymbol{q}}) - \boldsymbol{g}(\boldsymbol{q})) \\ & + \mathbf{B}^{-1}(\mathbf{D}_{\mathrm{m}}\dot{\boldsymbol{\theta}} - \boldsymbol{\tau}_{\mathrm{m}}) - \mathbf{H}(\mathbf{K}_{\mathrm{t}}(\boldsymbol{q} - \boldsymbol{\theta}) + \mathbf{D}_{\mathrm{t}}(\dot{\boldsymbol{q}} - \dot{\boldsymbol{\theta}}))\end{aligned} \tag{7}$$

Considering $\dot{q}_i = \dot{\theta}_i$ for $i = l_1, ..., l_{\mathrm{n}}$, the rows of (6) related to locked joints can be written as follows

$$\sum_{j=l_1,..,l_n} H_{i,j}\tau_{\mathrm{sf},j} + \sum_{j=u_1,..,u_n} H_{i,j}\tau_{\mathrm{df},j} = P_i, \tag{8}$$

where $H_{i,j}$ is the element of the $i$th row and $j$th column of $\mathbf{H}$. By rewriting (8) in matrix form, the friction torques associated with locked joints are obtained by

$$\boldsymbol{\tau}_{\mathrm{s}} = \mathbf{H}_{\mathrm{s}}^{-1}(\boldsymbol{\varphi} - \mathbf{H}_{\mathrm{d}}\boldsymbol{\tau}_{\mathrm{d}}), \tag{9}$$

where $\boldsymbol{\tau}_{\mathrm{s}} = [\tau_{\mathrm{sf},l_1}, ..., \tau_{\mathrm{sf},l_n}]^T \in \Re^{l_n}$ is the vector of static friction torques, $\boldsymbol{\tau}_{\mathrm{d}} = [\tau_{\mathrm{df},u_1}, ..., \tau_{\mathrm{df},u_n}]^T \in \Re^{u_n}$ is the vector of dynamic friction torques related to unlocked joints, the auxiliary vector $\boldsymbol{\varphi} \in \Re^{l_n}$ is defined by $\boldsymbol{\varphi} = [P_{l_1}, ..., P_{l_n}]$, the matrices $\mathbf{H}_{\mathrm{s}}$ and $\mathbf{H}_{\mathrm{d}}$ are

$$\mathbf{H}_{\mathrm{s}} = \begin{bmatrix} H_{l_1,l_1} & \dots & H_{l_1,l_n} \\ \vdots & \ddots & \vdots \\ H_{l_n,l_1} & \dots & H_{l_n,l_n} \end{bmatrix} \in \Re^{l_n\times l_n}, \tag{10}$$

$$\mathbf{H}_{\mathrm{d}} = \begin{bmatrix} H_{l_1,u_1} & \dots & H_{l_1,u_n} \\ \vdots & \ddots & \vdots \\ H_{l_n,u_1} & \dots & H_{l_n,u_n} \end{bmatrix} \in \Re^{l_n\times u_n}, \tag{11}$$

and the invertibility of $\mathbf{H}_{\mathrm{s}}$ is guaranteed as $\mathbf{H}$ is a positive-definite matrix, since it is the summation of the inverse of

two positive-definite matrices, and $\mathbf{H}_{\mathrm{s}}$ is a square sub-matrix of this positive-definite matrix, i.e. $\mathbf{H}$.

The friction torque of the each joint of the arm can be found in a way similar to that for a single clutch mechanism [24]. Hence, the torque $\boldsymbol{\tau}_{\mathrm{s}}$ transmitted by the clutch on joints with zero deflection velocity, i.e. $\dot{q}_i \neq \dot{\theta}_i$, needs to be compared with the maximum static friction torques $\boldsymbol{\tau}_{\mathrm{fmax}}$. For the $i$th joint, this threshold is defined as follow

$$\tau_{\mathrm{fmax},i} = F_{\mathrm{n},i}\mu_{\mathrm{s},i}R_i, \tag{12}$$

where $\mu_{\mathrm{s},i}$ is the coefficient of static coulomb friction of $i$th joint.

In summary, given $u_n$ joints with non-negligible[1] relative velocity of transmission sides, the friction torques of these unlocked joints are obtained from (4). However, to obtain the friction torque of other $l_n$ joints presenting negligible velocity between transmission sides, i.e. $|\dot{q}_i - \dot{\theta}_i| < \omega_{\mathrm{tol},i}$ for $i = l_1, ..., l_n$, the resultant torque applied on the clutch surfaces of $i$th joint, $\tau_{\mathrm{sf},i}$, needs to be firstly determined through (9) and to be compared with the maximum static friction torque. This condition can then be described by (for $i = 1, ..., n$)

$$\tau_{\mathrm{c},i} = \begin{cases} \tau_{\mathrm{sf},i} & \text{for } i = l_1, ..., l_n \text{ and } |\tau_{\mathrm{sf},i}| \leq \tau_{\mathrm{fmax},i} \\ \tau_{\mathrm{df},i} & \text{for } i = u_1, ..., u_n \text{ or } |\tau_{\mathrm{sf},i}| > \tau_{\mathrm{fmax},i}, \end{cases} \tag{13}$$

As for a special condition in which all joints are locked, i.e. $l_n = n$, the static friction torque vector equation, (9), can be simplified to [24]

$$\boldsymbol{\tau}_{\mathrm{s}}^{*} = \mathbf{N}\boldsymbol{\tau}_{\mathrm{e}} - \boldsymbol{h} - \mathbf{K}_{\mathrm{t}}(\boldsymbol{q} - \boldsymbol{\theta}), \tag{14}$$

with auxiliary vector $\boldsymbol{h}$ and matrix $\mathbf{N}$ which are defined by

$$\boldsymbol{h} = \mathbf{N}(\mathbf{M}\mathbf{B}^{-1}(\boldsymbol{\tau}_{\mathrm{m}} - \mathbf{D}_{\mathrm{m}}\dot{\boldsymbol{q}}) + \boldsymbol{c}(\boldsymbol{q}, \dot{\boldsymbol{q}}) + \boldsymbol{g}(\boldsymbol{q}) + \mathbf{D}_{\mathrm{l}}\dot{\boldsymbol{q}}), \tag{15}$$

$$\mathbf{N} = (\mathbf{I} + \mathbf{M}\mathbf{B}^{-1})^{-1}, \tag{16}$$

where $\mathbf{I}$ is the $n$-dimensional identity matrix. The invertibility of $(\mathbf{I}+\mathbf{M}\mathbf{B}^{-1})$ is guaranteed as $\mathbf{B}$ and $\mathbf{M}$ are positive definite matrices, thereby $\mathbf{M}\mathbf{B}^{-1}$ and its summation with any positive definite matrix are also positive definite.

## III. Control

The proposed control strategy aims to employ the clutch of actuation units to adjust the transmissibility of the actuation transmission system depending on the task requirements. The controller engages the clutch to accurately track the desired path when no external object/agent present; while it releases the clutch to intrinsically make the robot flexible as soon as a contact with the environment occurs to benefit from interaction-related advantages arising from the embedded elastic elements.

The clutch normal force is the principal control input which makes the system operate in one of the following modes:

a) Compliant mode: clutches are disengaged, $F_{n,i} = 0$ for $i = 1, ..., n$, and actuation units behave as SEAs.
b) Slip mode: clutches are engaged but the applied clutch force is not sufficiently high to lock the transmission system, thereby there is slippage between the clutch plates.
c) Rigid mode: clutches are engaged and transmission systems are locked, resulting in actuators performing similar to traditional rigid actuator.

To fulfill the terms of aforesaid control strategy, it would be desirable to employ rigid mode for contact-free motion to achieve high precision and to exploit compliant mode when the robot is in contact with environment. Furthermore, to conveniently satisfy the interaction prerequisites of the considered scenario, when the robot works in rigid mode, the maximum static force that it can exert should be limited as the actuators possess high output mechanical impedance in this mode that increases interaction force rapidly [25], while compliant mode permits better control of the interaction force [26]. This force condition can be expressed by

$$\|\boldsymbol{J}^{\#T}\boldsymbol{\tau}_{\mathrm{e}}\| \leq \ f_{max}, \tag{17}$$

where $\boldsymbol{J} \in \Re^{k\times\ n}$ shows the kinematic jacobian matrix in which $k$ is the dimension of the TCP workspace, and $f_{max}$ is the maximum admissible force. ($\|.\|$ symbolizes the second norm and the superscript "*#T*"denotes the transpose pseudo-inverse operation)

For a given maximum external torque, in case the normal force applied to the transmission clutch is the minimum amount required for locking it, the system works in rigid mode as far as the external torque does not exceed the maximum admissible value. As soon as the external torque threshold is violated, the operating mode of the robot intrinsically switches to slip mode and the system takes the advantage of inherit compliance. This characteristics of the system can be exploited for contact detection through monitoring the deflection change as deflection angles present constant values when the robot is working in rigid mode, while any interaction with environment disturbs this mode and activates slip mode demonstrating changes in joint deflection angles.

To apply the lowest clutch normal force needed for activating the rigid mode and keeping the transmission system of all joints locked, the resultant torque on the friction surfaces of each joint, $\tau_{\mathrm{sf},i}$, should be smaller than the maximum static friction torque $\tau_{\mathrm{sfmax},i}$, for $i = 1, ..., n$. To take the external force limit into account, the maximum admissible torques of joints resulting from interaction force, $\boldsymbol{\tau}_{\mathrm{e}}^{*}$, can be calculated by employing the optimization procedure introduced in [19]. As the right value of external torques associated with respecting contact force constraint (17) is computed, the minimum amount of the clutch force required for exploiting rigid mode, $\boldsymbol{F}_{\mathrm{n}}^{R}$, can be found as follows

$$\boldsymbol{F}_{\mathrm{n}}^{R} = \boldsymbol{\mu}_{\mathrm{s}}^{-1}\mathbf{R}^{-1}(|\boldsymbol{h} + \mathbf{K}_{\mathrm{t}}(\boldsymbol{q} - \boldsymbol{\theta})| + |\mathbf{N}\boldsymbol{\tau}_{\mathrm{e}}^{*}|), \tag{18}$$

where $\boldsymbol{\mu}_{\mathrm{s}} = diag(\mu_{\mathrm{s},1}, ..., \mu_{\mathrm{s},n})$ and $\mathbf{R} = diag(R_1, ..., R_n)$ are the diagonal matrices of the static coulomb friction

[1]Due to errors and noises in computation/measurement of the deflection velocity, a tolerance is applied for the velocity condition. This Parameter $\omega_{\mathrm{tol},i}$ is an arbitrarily small and positive value, that was set to $\omega_{\mathrm{tol}} = 10^{-3} rad/s$ in our case.

coefficients and geometrical constant factors of the clutches' plates, respectively; and $|.|$ denotes the absolute value operator functioning on the vector elements. It must be noted that, although constant friction coefficients were considered in this work, depending on the working circumstance, they can be also time-varying as the force reference is derived from an algebraic equation (18).

By setting the clutch force reference $\boldsymbol{F}_{\text{nd}}$ according to (18), the transmission slips as soon as the contact force reaches the admissible threshold, the presence of external object/agent is detected, and different reaction plans can be employed. Here, three strategies have been implemented:

i) Stop strategy: in case the external force applied to it reaches the maximum admissible force level, the robot stops tracking the trajectory and clutches are disengaged, i.e. $F_{\text{n},i} = 0$ for $i = 1, ..., n$. (This strategy can also change to execute a short backward motion.)
ii) Resume strategy: the robot stops executing the task until the external force is removed and then it resumes tracking the trajectory, while clutches are engaged according to (18).
iii) Task-execution strategy: the robot control the interaction force and at the same time it continues executing the task in contact-free directions while clutches are disengaged, i.e. $F_{\text{n},i} = 0$ for $i = 1, ..., n$.

## IV. Experiments

### A. Experimental System Description

To evaluate the performance of proposed approach, experiments have been carried out on a compliant manipulator [27] presented in Fig. 3, CompAct™ arm. The Kinematic parameters of the arm, the range of motion (ROM) and homing position (HP) are presented in Table I. It is a light-weight anthropomorphic 4-DOF arm powered by compliant actuators equipped with friction clutches implemented in parallel to the passive elastic elements of each driving unit [28], see Fig. 2. Each clutch is comprised of an even steel plate acting against a friction ring made of Kevlar fiber. This mechanism is actuated by means of four Noliac SCMAP04 piezoelectric actuators placed in parallel to the axis of the motor.

The stiffness of joints are specified using the approach proposed in [29]; setting that of first two joints to 188 N.m/rad, and that of last two joints to 103 Nm/rad. The motor position is measured using a 12-bit encoder on the motor side. The transmission angle, which is particularly employed for contact detection, is also measured using a 12-bit encoder. Lower level control schemes including PD motor position controllers and PI Piezoelectric force controllers are implemented on custom-made digital signal processing (DSP) driver boards. Data acquisition of the system states at the DSP drivers was running at a rate of 1 kHz. Communication between the lower level drivers and control and the higher level controller, which was implemented on a PC104 machine using hard real-time version of Linux (Xenomai), was executed also at 1 kHz. The higher level controller is

TABLE I: DH Parameters of the arm presented in Fig. 3

| $i$ | $\alpha_i$ | $a_i$ | $d_i$ | $\theta_i$ | ROM | HP |
|---|---|---|---|---|---|---|
| 1 | $\pi/2$ | 0 | 0.262 | $q_1 - \pi/2$ | [-45,180]° | 0° |
| 2 | $\pi/2$ | 0 | 0 | $q_2 - \pi/2$ | [0,170]° | 0° |
| 3 | $\pi/2$ | 0.096 | 0.430 | $q_3 - \pi/2$ | [-90,90]° | 0° |
| 4 | 0 | 0.459 | 0 | $q_4 - \pi/2$ | [0,145]° | 90° |

comprised of the motor position trajectory generator, clutch reference force calculator and contact detection block.

Defining three dimensional position trajectories excluding the orientation of TCP, $\boldsymbol{X} = [X, Y, Z]^T$, the inverse kinematics problem is solved via exploiting one degree of motion redundancy for either respecting joint limits or minimizing joint velocities [30]. The desired link position $\boldsymbol{q}_{\text{d}}$ is therefore updated by

$$\delta \boldsymbol{q}_{\text{d}} = \boldsymbol{J}^{\#} \delta \boldsymbol{X}_{\text{d}} - \alpha (\mathbf{I} - \boldsymbol{J}^{\#} \boldsymbol{J}) (\frac{\partial \phi}{\partial \boldsymbol{q}_{\text{d}}})^T, \tag{19}$$

where $\alpha$ is a positive constant that was set to $\alpha = 0.01$ in our system, $\delta$ denotes variation operator, and $\phi$ is the potential function defined based on avoiding reaching joint limits which is specified by

$$\phi = \sum_{i=1}^{4} \left( \frac{q_{\text{d},i} - q_{\text{mid},i}}{q_{\text{max},i} - q_{\text{min},i}} \right)^2, \tag{20}$$

in which $q_{\text{mid},i}$ is the middle value of the joint range, and $q_{\text{max},i}$ and $q_{\text{min},i}$ are maximum and minimum joint limits, respectively.

In case the robot operates in "compliant mode", using the gravity compensator proposed for robots with elastic joints [31], the desired motor position is obtained from $\boldsymbol{\theta}_{\text{d}} = \boldsymbol{q}_{\text{d}} + \mathbf{K}_{\text{t}}^{-1} \boldsymbol{g}(\boldsymbol{q}_{\text{d}})$. However, the employment of the "rigid mode" makes the transmission locked and suspend the effects of passive elasticity on tracking performance. As a result of that, the motor position can be computed from $\boldsymbol{\theta}_{\text{d}} = \boldsymbol{q}_{\text{d}} + \boldsymbol{d}$ in which $\boldsymbol{d}$ is the constant difference between motor and link position of joints since there will be a constant difference between motor and link angles if springs are deflected before locking the transmission. Hence, this constant offset, i.e. $\boldsymbol{d}$, needs to be taken at the first moment joints get locked.

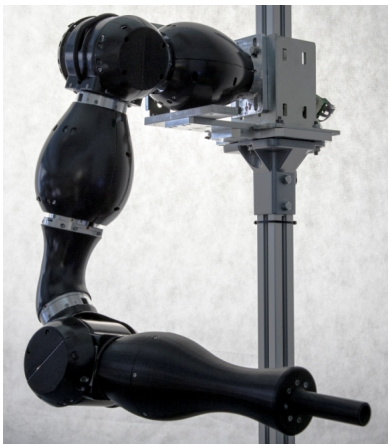

Fig. 3: A picture of CompAct™ arm used for experiments.

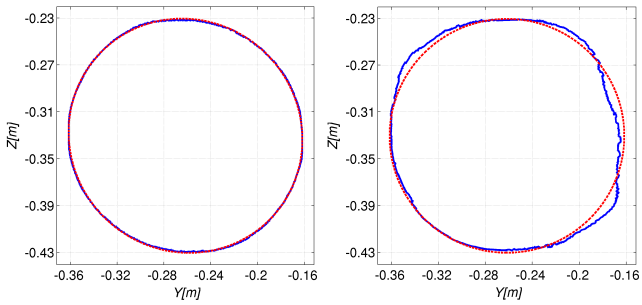


(a) (b)

Fig. 4: The desired Cartesian path of the end-effector (−−) compared to the real path (−) tracked in (a) rigid mode; (b) compliant mode.

As it was discussed in Section III, the force reference is computed from (18) for a given maximum admissible force threshold as far as rigid mode motion is desired. However, in case "Stop strategy" or "Task-execution strategy" are desired, the clutch force reference switches to zero as soon as the external force reaches the admissible threshold. While the "rigid mode" is active, changes in transmission angles of joints are monitored. The interaction/collision is detected when the change of the passive deflection angle of a joint exceeds a defined level that is considered to ignore the effects of noise and corresponds to 1 bit resolution (0.0015 rad).

### B. Experimental Results

*1) Trajectory Tracking:* This experiment was carried out to demonstrate the effectiveness of the friction clutches in improving the tracking performance. A circular path is considered as the position reference. The desired position $\boldsymbol{X}_{\mathrm{d}}$ is defined by

$$\boldsymbol{X}_{\mathrm{d}} = \boldsymbol{X}_0 + [0 \;\; 0.1sin(1.6\pi t) \;\; 0.1(1-cos(1.6\pi t))]^T \mathrm{m} \quad (21)$$

where $\boldsymbol{X}_0 = [0.555, -0.262, -0.430]^T$ m is the initial posture configuration of the arm at homing position as shown in Fig. 3.

Fig. 4 shows the results of trajectory tracking tasks for the robot operating in two different working modes: in Compliant mode without engaging the clutches and in Rigid mode applying the clutch force according to (18). It is observed that the tracking performance of the robot can be considerably improved by implementing the rigid mode.

*2) Contact Detection:* These experiments were carried out to demonstrate the effectiveness of the interaction detection scheme while the robot collides against soft and stiff surfaces, see Fig. 5. The regulation of the force applied on the clutch for rigid mode motion is performed by considering a null maximum external force $f_{\max} = 0$ N to achieve the highest sensitivity to external forces/torques. The considered trajectory for this experiment is a straight horizontal line in Y-axis with the constant velocity 0.4m/s, i.e. $\boldsymbol{X}_{\mathrm{d}} = \boldsymbol{X}_0 + [0 \;\; 0.4t \;\; 0]^T$ m, while the Stop reaction strategy is implemented, see Sec. III. Change in the transmission angles of joints and contact forces generated during the interaction

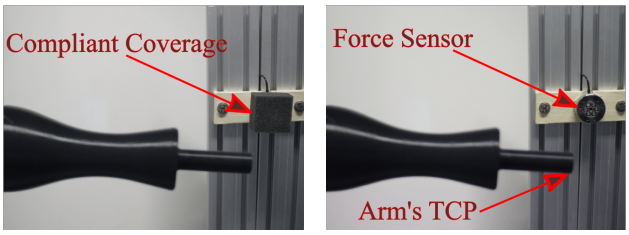


(a) (b)

Fig. 5: Experimental setup. The arm's end-effector colliding with (a) soft surface made of foam; (b) stiff surface.

are illustrated in Fig. 6. As it can be seen in soft and stiff interactions, the interaction is promptly detected according to the scheme discussed in Sec. III, and the exerted force is merely due to impact effect. It can be seen that the level of generated peak force is different in two scenarios which could be predicted as the force transmissibility is much higher in case of stiff contact between the TCP and the obstacle, shown in Fig. 6c. Results in Fig. 6a demonstrates that the maximum TCP static force can be effectively limited by means of the proposed approach. However, the minimum force level which triggers collision is approximately 3 N.

## V. Conclusion

This work presented a novel control strategy for compliant manipulators equipped with transmission friction clutches placed in parallel to the passive elastic elements of each actuation unit. By modulating the normal clutch force, three different operating modes can be achieved which are exploited for various operating conditions. Particularly, the clutch mechanism can be controlled to make the robot perform as a rigid or compliant manipulator based on the task demands to

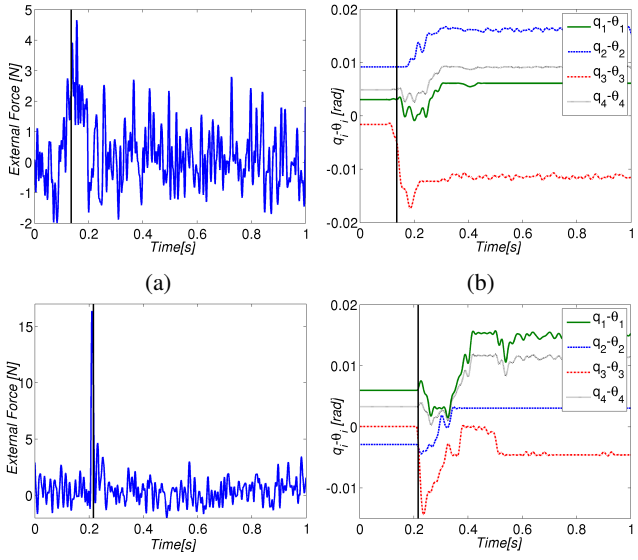


(a) (b)

(c) (d)

Fig. 6: Time history of joints deflection angles (b and d) and measured contact force in collision with (a) soft and (c) stiff contact surface. (vertical line (−) shows contact detection instant)

accommodate precision or interaction performance, respectively. To optimize the mentioned interaction/performance trade-off, a strategy has been formulated to control the force applied to the clutches when the manipulator is operating in rigid mode. The generated external force during the interaction is limited to a maximum threshold which is defined by the user depending on the task. Preliminary experimental results carried out on the CompAct™ arm [27] show that, apart from improving the tracking performance, the clutches can be exploited to use robot in rigid configuration without significantly affecting the contact forces during interaction thanks to the proposed control approach. This makes it possible to exploit the advantages of rigid robots while at the same time benefiting from the advantages offered by compliance in interaction scenarios by switching to compliant mode. Furthermore, the employment of proposed approach for contact detection was demonstrated.

## ACKNOWLEDGMENT

Authors would like to thank Gianluca Pane for the help on the identification of system parameters, and Jinoh Lee for useful discussions.

This work is supported by the European Commission project SAPHARI FP7-ICT-287513.

## REFERENCES

[1] A. M. Dollar and R. D. Howe, "A robust compliant grasper via shape deposition manufacturing," *Mechatronics, IEEE/ASME Transactions on*, vol. 11, no. 2, pp. 154–161, 2006.

[2] N. Vitiello, T. Lenzi, J. McIntyre, S. Roccella, E. Cattin, F. Vecchi, and M. C. Carrozza, "Characterization of the NEURARM bio-inspired joint position and stiffness open loop controller," in *Biomedical Robotics and Biomechatronics, 2008. BioRob 2008. 2nd IEEE RAS & EMBS International Conference on*. IEEE, 2008, pp. 138–143.

[3] G. A. Pratt and M. M. Williamson, "Series elastic actuators," in *Intelligent Robots and Systems 95. 'Human Robot Interaction and Cooperative Robots', Proceedings. 1995 IEEE/RSJ International Conference on*, vol. 1, 1995, pp. 399–406 vol.1.

[4] N. G. Tsagarakis, S. Morfey, G. Medrano Cerda, L. Zhibin, and D. G. Caldwell, "Compliant humanoid coman: Optimal joint stiffness tuning for modal frequency control," in *Robotics and Automation (ICRA), 2013 IEEE International Conference on*. IEEE, 2013, pp. 673–678.

[5] M. Zinn, B. Roth, O. Khatib, and J. K. Salisbury, "A new actuation approach for human friendly robot design," *International Journal of Robotics Research*, vol. 23, no. 4-5, pp. 379–398, 2004.

[6] L. Chen, M. Garabini, M. Laffranchi, N. Kashiri, N. G. Tsagarakis, A. Bicchi, and D. G. Caldwell, "Optimal Control for Maximizing Velocity of the CompAct Compliant Actuator," in *Robotics and Automation (ICRA), 2013 IEEE International Conference on*, Karlsruhe (Germany), 2013, pp. 516–522.

[7] M. Laffranchi, N. G. Tsagarakis, and D. G. Caldwell, "Analysis and Development of a Semiactive Damper for Compliant Actuation Systems," *Mechatronics, IEEE/ASME Transactions on*, 2012.

[8] F. Petit and A. Albu-Schaffer, "State feedback damping control for a multi DOF variable stiffness robot arm," *Robotics and Automation (ICRA), 2011 IEEE International Conference on*, pp. 5561–5567, 2011.

[9] A. Radulescu, M. Howard, D. J. Braun, and S. Vijayakumar, "Exploiting variable physical damping in rapid movement tasks," in *Advanced Intelligent Mechatronics (AIM), 2012 IEEE/ASME International Conference on*. IEEE, 2012, pp. 141–148.

[10] M. Laffranchi, N. G. Tsagarakis, and D. G. Caldwell, "A variable physical damping actuator (VPDA) for compliant robotic joints," in *Robotics and Automation (ICRA), 2010 IEEE International Conference on*. IEEE, 2010, pp. 1668–1674.

[11] M. Laffranchi, L. Chen, N. G. Tsagarakis, and D. G. Caldwell, "The role of physical damping in compliant actuation systems," in *2012 IEEE/RSJ International Conference on Intelligent Robots and Systems*. IEEE, Oct. 2012, pp. 3079–3085.

[12] C. English and D. Russell, "Implementation of variable joint stiffness through antagonistic actuation using rolamite springs," *Mechanism and Machine Theory*, vol. 34, no. 1, pp. 27–40, Jan. 1999.

[13] R. Van Ham, B. Vanderborght, M. Van Damme, B. Verrelst, and D. Lefeber, "MACCEPA: the actuator with adaptable compliance for dynamic walking bipeds," in *Climbing and Walking Robots*. Springer, 2006, pp. 759–766.

[14] A. Jafari, N. G. Tsagarakis, and D. G. Caldwell, "A Novel Intrinsically Energy Efficient Actuator With Adjustable Stiffness (AwAS)," *Mechatronics, IEEE/ASME Transactions on*, vol. 18, no. 1, pp. 355–365, 2013.

[15] E. J. Rouse, L. M. Mooney, E. C. Martinez-Villalpando, and H. M. Herr, "Clutchable Series-Elastic Actuator: Design of a Robotic Knee Prosthesis for Minimum Energy Consumption," in *International Conference on Rehabilitation Robotics*, 2013.

[16] M. Catalano, G. Grioli, M. Garabini, F. W. Belo, A. di Basco, N. Tsagarakis, and A. Bicchi, "A Variable Damping Module for Variable Impedance Actuation," in *Robotics and Automation (ICRA), 2012 IEEE International Conference on*. IEEE, 2012, pp. 2666–2672.

[17] A. Enoch, A. Sutas, S. Nakaoka, and S. Vijayakumar, "BLUE: A Bipedal Robot with Variable Stiffness and Damping," in *Humanoid Robots (Humanoids), 2012 12th IEEE-RAS International Conference on*, Osaka, 2012, pp. 487–494.

[18] H. Tomori, Y. Midorikawa, and T. Nakamura, "Derivation of nonlinear dynamic model of novel pneumatic artificial muscle manipulator with a magnetorheological brake," in *Advanced Motion Control (AMC), 2012 12th IEEE International Workshop on*, 2012, pp. 1–8.

[19] N. Lauzier and C. Gosselin, "Series Clutch Actuators for safe physical human-robot interaction," in *Robotics and Automation (ICRA), 2011 IEEE International Conference on*. IEEE, 2011, pp. 5401–5406.

[20] S. Morinaga and K. Kosuge, "Collision detection system for manipulator based on adaptive impedance control law," in *Robotics and Automation, 2003. Proceedings. ICRA'03. IEEE International Conference on*, vol. 1. IEEE, 2003, pp. 1080–1085.

[21] A. De Luca and R. Mattone, "Sensorless robot collision detection and hybrid force/motion control," in *Robotics and Automation, 2005. ICRA 2005. Proceedings of the 2005 IEEE International Conference on*. IEEE, 2005, pp. 999–1004.

[22] S. Haddadin, A. Albu-Schaffer, A. De Luca, and G. Hirzinger, "Collision detection and reaction: A contribution to safe physical human-robot interaction," in *Intelligent Robots and Systems, 2008. IROS 2008. IEEE/RSJ International Conference on*. IEEE, 2008, pp. 3356–3363.

[23] M. W. Spong, "Modeling and Control of Elastic Joint Robots," *Journal of Dynamic Systems, Measurement, and Control*, vol. 109, no. 4, pp. 310–318, Dec. 1987.

[24] N. Kashiri, M. Laffranchi, N. G. Tsagarakis, I. Sardellitti, and D. G. Caldwell, "Dynamic modeling and adaptable control of the CompAct arm," in *Mechatronics (ICM), 2013 IEEE International Conference on*, 2013, pp. 477–482.

[25] T. G. Sugar and V. Kumar, "Design and control of a compliant parallel manipulator," *Journal of Mechanical Design*, vol. 124, p. 676, 2002.

[26] J. Pratt, B. Krupp, and C. Morse, "Series elastic actuators for high fidelity force control," *Industrial Robot: An International Journal*, vol. 29, no. 3, pp. 234–241, 2002.

[27] M. Laffranchi, N. G. Tsagarakis, and D. G. Caldwell, "CompAct Arm: a Compliant Manipulator with Intrinsic Variable Physical Damping," *Robotics: Science and Systems VIII*, p. 225, 2013.

[28] M. Laffranchi, N. Tsagarakis, and D. G. Caldwell, "A compact compliant actuator (CompAct) with variable physical damping," in *Robotics and Automation (ICRA), 2011 IEEE International Conference on*. IEEE, 2011, pp. 4644–4650.

[29] N. Kashiri, N. G. Tsagarakis, M. Laffranchi, and D. G. Caldwell, "On the stiffness design of intrinsic compliant manipulators," in *Advanced Intelligent Mechatronics (AIM), 2013 IEEE/ASME International Conference on*. IEEE, 2013, pp. 1306–1311.

[30] Y. Nakamura, *Advanced robotics: redundancy and optimization*. Addison-Wesley Longman Publishing Co., Inc., 1990.

[31] P. Tomei, "A simple PD controller for robots with elastic joints," *Automatic Control, IEEE Transactions on*, vol. 36, no. 10, pp. 1208–1213, 1991.